# Two-Element Mixture of Bose and Fermi Superfluids

Richard Roy, Alaina Green, Ryan Bowler, and Subhadeep Gupta
*Department of Physics, University of Washington, Seattle, Washington 98195, USA*

(Received 11 July 2016; revised manuscript received 4 November 2016; published 2 February 2017)

We report on the production of a stable mixture of bosonic and fermionic superfluids composed of the elements $^{174}$Yb and $^{6}$Li which feature a strong mismatch in mass and distinct electronic properties. We demonstrate elastic coupling between the superfluids by observing the shift in dipole oscillation frequency of the bosonic component due to the presence of the fermions. The measured magnitude of the shift is consistent with a mean-field model and its direction determines the previously unknown sign of the interspecies scattering length to be positive. We also observe the exchange of angular momentum between the superfluids from the excitation of a scissors mode in the bosonic component through interspecies interactions. We explain this observation using an analytical model based on superfluid hydrodynamics.

DOI: 10.1103/PhysRevLett.118.055301

Ultracold atomic gases offer excellent opportunities to produce and investigate quantum matter, allowing fundamental studies in many-body physics and quantum simulation [1]. Beginning with the cooling of atoms to Bose-Einstein condensation [2,3] and later followed by the achievement of superfluidity in atomic Fermi gases [4], such studies have found many parallels with the analogous superfluids of bosonic $^{4}$He and fermionic $^{3}$He as well as superconductors, familiar from condensed matter physics. While the goal of simultaneous superfluidity in mixtures of $^{4}$He-$^{3}$He still remains elusive due to strong interisotope interactions [5,6], Bose-Fermi superfluidity in an atomic gas isotopic mixture of $^{7}$Li-$^{6}$Li has recently been realized [7]. The original interest [8,9] in such dual superfluid systems is now strongly intensified [10–16].

The extension of Bose-Fermi superfluidity to mixtures of different elements is experimentally challenging, but holds the potential to open a larger arena of scientific studies. A large mass ratio between the components is predicted to alter the interaction energy between the superfluids [12] as well as the character of excitations across the Bose-Einstein condensate to Bardeen-Cooper-Schreiffer (BEC-BCS) crossover for the fermion pairs [15]. Specific interaction strengths and mass ratios can aid the detection of exotic states such as the Fulde-Ferrell-Larkin-Ovchinnikov (FFLO) phase [10] and dark-bright solitons [16]. Furthermore, species-selective potentials for relative positioning and selective addressing make two-element systems more amenable for systematic studies.

In this Letter, we report on the realization of a two-element Bose-Fermi superfluid mixture of $^{174}$Yb-$^{6}$Li. We measure their coupling by observing the interaction-induced frequency shift of the bosonic dipole mode. We also detect transfer of angular momentum between the superfluids through the excitation of a scissors mode in the bosonic component. The scattering length $a_F$ of the two-spin alkali $^{6}$Li fermionic system is tunable across the BEC-BCS crossover through a Feshbach resonance centered at 832 G, while the scattering length $a_B$ of the alkaline-earth-like bosonic Yb remains constant throughout. The combination of spin-half (Li, $^{2}S_{1/2}$) and spin-zero (Yb, $^{1}S_{0}$) electronic states allows external magnetic fields to be used as a convenient species-specific tool and results in a uniform interspecies scattering length $a_{BF}$ for all Li spin states.

The preparation of the dual superfluid involves significant extensions to our earlier cooling methods for the dual-species Yb-Li system [17] (see Supplemental Material [18]). Briefly, we load laser-cooled atoms into a crossed-beam 1064 nm optical dipole trap (ODT) optimized for efficient evaporative cooling by dynamically changing the trap shape [28]. The relative polarizability and trap frequency of the bosonic and fermionic components are $\alpha_F/\alpha_B = 2.2$ and $\omega_F/\omega_B = 8$. We perform forced evaporative cooling of Yb and simultaneous sympathetic cooling of a single spin state of Li to quantum degeneracy at $B = 330$ G, achieving a mixture of up to $3 \times 10^5$ Yb atoms in a pure condensate and $2 \times 10^5$ Li atoms with $T/T_F \leq 0.2$.

At this stage, the Yb trap frequencies are $(\omega_x, \omega_y, \omega_z)_B = 2\pi \times (23, 150, 10)$ Hz, where gravity points in the $-y$ direction. For these parameters, the two species are thermally decoupled with cloud centers separated by $y_{0,F} - y_{0,B} = 11$ $\mu$m due to the large differential gravitational sag stemming from the large mass mismatch.

To proceed towards pairing and condensation of the Fermi gas, we exploit the different electronic character of Yb and Li and individually address Li with external magnetic fields. First, we bring the system to 832 G and prepare a 50:50 spin mixture of Li in the two lowest hyperfine states, $|1\rangle$ and $|2\rangle$, using a radio-frequency (rf) pulse, and allow the resulting equal superposition state to decohere over 100 ms. The magnetic insusceptibility of Yb ensures stability of the BEC at all magnetic fields as the trapping potential and $a_B = 5.6$ nm remain unchanged.

 

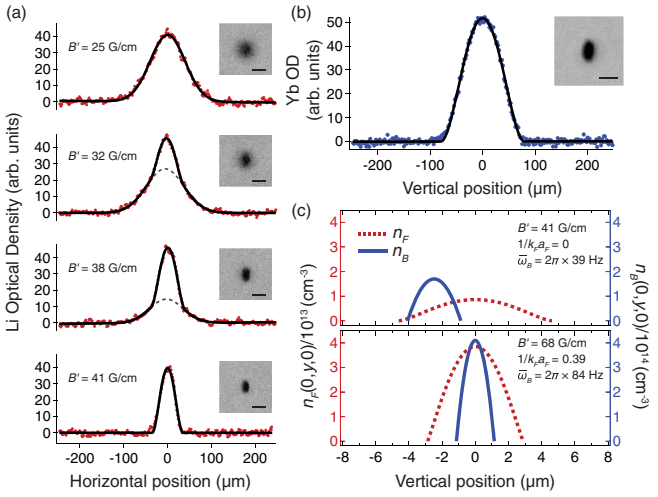


FIG. 1. (a) Gradient controlled forced evaporative cooling of a Li unitary Fermi gas. We image the atoms at 690 G with 2 ms TOF (scale bar is 100 $\mu$m). Solid lines are bimodal fits to doubly integrated optical density (OD) profiles, with dashed lines indicating the thermal component. From top to bottom, the detected condensate fractions $f_c$ are 0, 0.2, 0.5, and $\geq 0.85$. (b) Yb BEC of $1.1 \times 10^5$ (30 ms TOF) atoms coexisting with a Li superfluid of $0.8 \times 10^5$ atoms. Solid line is a fit to a pure Thomas-Fermi BEC profile. Gravity is in the vertical direction for all images in (a) and (b). (c) Calculated in-trap fermionic (dashed red lines) and bosonic (solid blue line) superfluid density profiles for (upper panel) the combined superfluid lifetime measurement at unitarity and (lower panel) the bosonic dipole oscillation measurements at 780 G presented in Fig. 2. For the fermion we use the zero-temperature EOS $n_F(\mu_F, a_F)$ and the local density approximation to obtain $n_F(\vec{r})$ [18,30], and for the boson a pure BEC profile in the Thomas-Fermi limit. The gradient of $B' = 41$ G/cm ensures complete overlap of the two clouds, while $B' = 68$ G/cm guarantees $y_{0,B} = y_{0,F}$.

Next we perform independent forced evaporative cooling of Li at 832 G using a magnetic field gradient $B'$ in the vertical direction [29]. This gradient reduces the trap depth for Li and moves the cloud center towards the Yb BEC. Typically, we ramp $B'$ from zero to its final value over 500 ms, and hold for 200 ms. To perform thermometry of Li, we ramp the magnetic field in trap from 832 G to 690 G, where $1/k_Fa_F = 2.9$, in 5 ms, and image the resulting molecular cloud in time of flight (TOF). Here $k_F = \sqrt{2m_FE_F}/\hbar$ is the Fermi wave vector and $k_BT_F = E_F = \hbar\bar{\omega}_F(3N_F)^{1/3}$ the Fermi energy of a harmonically trapped, spin-balanced Fermi gas with $N_F$ atoms and geometric mean trap frequency $\bar{\omega}_F$. Figure 1(a) displays a progression for different final $B'$ values towards the detection of a molecular BEC consisting of $0.4 \times 10^5$ molecules and no detectable thermal component, coexisting with a pure Yb superfluid of $1.1 \times 10^5$ atoms [Fig. 1(b)] with an applied gradient of $B' = 41$ G/cm providing strong interspecies cloud overlap [18].

We infer superfluidity of the Fermi gas at unitarity by comparing the observed entropy of the molecular BEC with the equation of state (EOS) of the unitary Fermi gas [31,32]. Importantly, we observe no difference in molecular condensate fraction $f_c$ if we remove the gradient $B'$ before ramping from 832 G to 690 G. For $B' = 41$ G/cm, we estimate that removing the gradient increases the trap depth for Li by a factor of 6. We also observe the same $f_c$ if Yb is removed with a resonant pulse of light immediately before the ramp. Consequently, we conclude that no evaporative or sympathetic cooling occurs during the ramp to the weakly interacting BEC regime for the measurements in Fig. 1(a). Therefore, the observed entropy of the molecular BEC gives an upper bound on the entropy of the initial unitary Fermi gas, since the ramp is at best adiabatic.

To determine the entropy of the molecular condensate at 690 G, we calculate the relevant quantities in the Thomas-Fermi limit. This is justified since $n_m(0)a_m^3 = 0.001$, where $n_m(0)$ is the peak molecular BEC density and $a_m = 0.6a_F$ is the molecule-molecule scattering length [33]. The thermal fraction of the coldest Li clouds is below our detection limit of $1 - f_c = 0.15$, implying that the total entropy in the trap, including the effects of interactions [18,34], is $S/(N_Fk_B) \leq 0.55$, which is well below the critical entropy for a unitary Fermi gas at the superfluid transition in a harmonic trap $S_c/(N_Fk_B) = 1.70$ [31]. The measurements in Ref. [31] determine the EOS $S(T/T_F)$ for trap-averaged reduced temperatures above $T/T_F = 0.15$, at which point $S/(N_Fk_B) = 0.92$, and are thus not applicable at our measured entropy. If instead we compare with the EOS calculated in Ref. [32], which agrees well with Ref. [31], we determine an upper bound on the temperature at unitarity of $T \leq 0.12T_F = 0.55T_{c,F}$, where $T_{c,F} = 0.22T_F$ is the critical temperature for superfluidity at unitarity in a harmonic trap [18].

To measure the stability of the dual superfluid at unitarity, we first adiabatically increase the ODT power by 50% to inhibit evaporation and subsequently hold the overlapped clouds in the trap for a variable time at 832 G before ramping to 690 G and imaging in TOF. The upper panel in Fig. 1(c) depicts the relative Bose and Fermi superfluid density profiles in the vertical dimension for this situation. From exponential fits to the observed condensate number evolution we determine lifetimes of 1.8 s and 0.7 s for Yb and Li, respectively.

The Yb-Li dual superfluid system features a small BEC inside a larger Fermi superfluid. For the lifetime measurements at unitarity discussed above, the relative in-trap cloud radii are $R_B/R_F = 0.36$, where $R_\beta = (2\mu_\beta/m_\beta\bar{\omega}_\beta^2)^{1/2}$ for $\beta = B$ and $F$, $\mu_F = \sqrt{\xi}E_F$ is the chemical potential for a zero-temperature unitary Fermi gas, $\xi = 0.37$ is the Bertsch parameter [31,35], and $\mu_B$ is the chemical potential for the Yb BEC. Additionally, the effects of interspecies mean-field interactions are small, with $V_{BF(FB)}(0)/\mu_{F(B)} = 0.07(0.14)$, where $V_{BF(FB)}(0)$ is the peak interspecies mean field interaction energy of Yb on Li (Li on Yb).

To probe elastic interactions in the dual superfluid we selectively excite vertical center-of-mass (dipole)

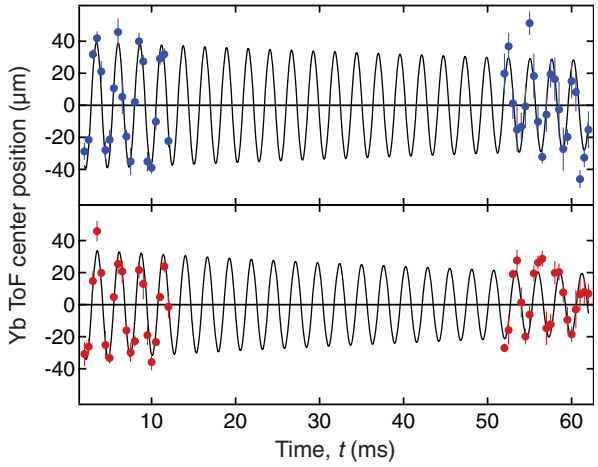


FIG. 2. Yb BEC dipole oscillations without (blue circles, upper panel) and with (red circles, lower panel) the Li superfluid at 780 G. Center-of-mass position measured at 30 ms TOF (solid lines are fits, see text).

oscillations in the bosonic component and measure the oscillation frequency with and without the presence of the overlapped fermionic component [7]. Because of the large ratio of trap frequencies for Li and Yb, we can achieve this species-selective excitation by increasing the trapping laser power $P$ on a time scale that is diabatic (adiabatic) for Yb (Li), where the diabatic excitation arises from the power-dependent gravitational sag, $y_{0,B} \propto 1/P$. Prior to the Yb excitation, we increase the magnetic gradient to the value $B' = 68$ G/cm that ensures $y_{0,F} = y_{0,B}$ [Fig. 1(c), lower panel], concurrent with an adiabatic increase of $P$ to prevent spilling of Li due to the strong gradient.

Figure 2 shows dipole oscillation measurements of the Yb BEC with and without the Fermi superfluid at 780 G, where $1/k_F a_F = 0.39$. We perform these measurements at 780 G instead of 832 G in order to enhance the effect of Li on the Yb oscillations [7]. For these measurements, after the species-selective excitation, the superfluids are held in a trap with $(\omega_x, \omega_y, \omega_z)_B = 2\pi \times (59, 388, 26)$ Hz for a variable time $t$ before TOF imaging [36]. During the 30 ms TOF for Yb, the in-trap momentum oscillation converts into an oscillation of the vertical position. For the measurements without Li, we keep the experimental preparation of the dual superfluid the same, and remove the fermionic component by spilling with a strong gradient before initiating the dipole oscillation.

We fit exponentially damped sinusoids to the measurements in Fig. 2 and extract $\omega_{y,B}/2\pi = 387.7(3)$ Hz (without Li) and $\omega'_{y,B}/2\pi = 381.3(4)$ Hz (with Li), yielding a reduction of the dipole oscillation frequency of 1.7(2)%. From the amplitude of the oscillation in TOF, we determine the maximum in-trap velocity and displacement to be 1.2 mm/s and 0.5 $\mu$m for the Yb BEC with a vertical Thomas-Fermi radius $R_{B,y} = 1.1$ $\mu$m. The small amplitude of oscillation ensures that the Bose probe remains well localized inside the larger Fermi cloud [Fig. 1(c), lower panel].

From the decay constant $\tau$ for the oscillations with Li, we find that $\omega'_{y,B}\tau = 250$, which ensures that our determination of the dipole frequency is unaffected by the decay. The finite quality factor is most likely due to anharmonicities of the ODT potential, as the damping times with and without Li are within error of each other. While the maximum Yb velocity is an order of magnitude below the critical velocity of this Bose-Fermi superfluid system [15,37], we cannot rule out the possibility of dissipation due to a finite Li thermal component.

To model the effect of Li on the Yb dipole oscillations, we adopt a mean-field treatment, in which Yb experiences an effective potential $V_B(\vec{r}) = V_{T,B}(\vec{r}) + g_{BF} n_F(\vec{r})$, where $V_{T,B}(\vec{r})$ is the Yb optical potential, $g_{BF} = 2\pi\hbar^2 a_{BF}/m_{BF}$, $m_{BF}$ is the Yb-Li reduced mass, and $n_F(\vec{r})$ is the fermion density. In the local density approximation, the spatial curvature of the Fermi superfluid density gives rise to a shift of the bosonic dipole oscillation frequency given by [7]

$$\frac{\delta\omega_{y,B}}{\omega_{y,B}} = -\frac{g_{BF}}{2}\frac{\alpha_F}{\alpha_B}\frac{dn_F}{d\mu_F}\bigg|_{\mu_F(0)}. \quad (1)$$

Here $\delta\omega_{y,B} = \omega'_{y,B} - \omega_{y,B}$, $\mu_F(\vec{r}) = \mu_F(0) - V_{T,F}(\vec{r})$ is the local chemical potential, and $V_{T,F}(\vec{r}) = (\alpha_F/\alpha_B)V_{T,B}(\vec{r})$ is the Li optical potential. Using the magnitude of $a_{BF}$ derived from interspecies thermalization measurements [38,39], $|a_{BF}| = 15(2)a_0$ [40], this model predicts a frequency shift at $1/k_F a_F = 0.39$ of absolute value 2.0(3)%. The uncertainty in the prediction comes entirely from the uncertainty in the measurement of $|a_{BF}|$. The predicted magnitude is in good agreement with the measurement in Fig. 2, and the direction of the observed frequency shift determines the previously unknown sign of the Yb-Li $s$-wave scattering length to be positive.

The mean field interaction exerted on the fermions by the oscillating BEC also modulates the potential felt by the fermions. However, due to the large value of $\omega_F/\omega_B$, this modulation can be adiabatically followed by Li. Consistent with this picture, we observe no motion from backaction on Li.

The shift in the dipole oscillation frequency clearly demonstrates the coupling between the two superfluids. Additionally, we observe a modulation of the angular orientation of the Yb BEC due to interactions with Li. Our observations are shown in Figs. 3(b) and 3(c), where we plot the tilt angle $\theta_{B,\mathrm{TOF}}$ of the Yb BEC at 30 ms TOF for the same data set used in Fig. 2. The presence of Li leads to a modulation of this angle during the dipole oscillation. By fitting the measurements with Li to a pure sine wave, we extract a tilt angle modulation frequency of $\omega_\theta/\omega'_{y,B} = 1.02(3)$, with a modulation amplitude of 1.3(3) degrees and phase at $t = 0$ of $\phi = 0.6 \pm 0.5$ rad. The amplitude of

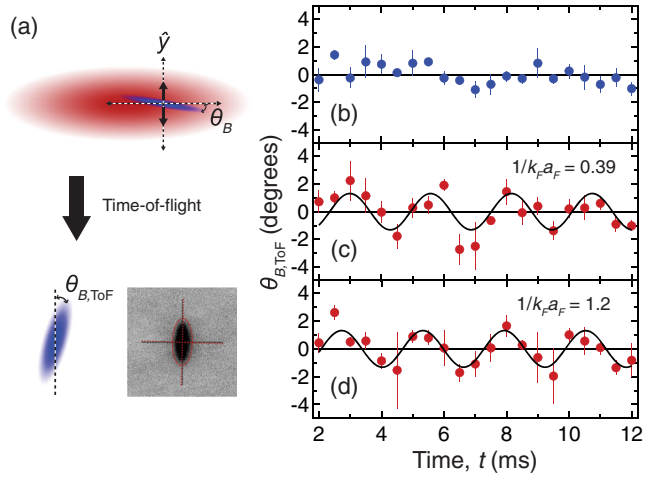


FIG. 3. (a) While executing dipole oscillations along $\hat{y}$, the tilt angle of the Yb BEC $\theta_B$ exhibits a modulation due to interactions with the horizontally offset Li superfluid. This in-trap angle modulation maps proportionally to a tilt $\theta_{B,\mathrm{TOF}}$ for long TOF. In the absorption image, the red axes are aligned to the major and minor axes of the BEC tilted 1.3° clockwise with respect to the trap eigenaxes (black). (b) Tilt angle measurements in the absence of Li. (c) and (d) Observation of a scissors mode excitation in Yb due to interaction with Li at 780 G ($1/k_F a_F = 0.39$) and 720 G ($1/k_F a_F = 1.2$).

a fit to the data without Li is consistent with zero modulation. Similar behavior is observed at 720 G [Fig. 3(d)] where $1/k_F a_F = 1.2$, with the fit returning a modulation frequency of $\omega_\theta/\omega'_{y,B} = 1.01(3)$, with an amplitude of 1.3(3) degrees and phase of $\phi = 1.3 \pm 0.6$ rad. For each field, we present the frequency measurement as a ratio with respect to the mean-field-shifted frequency $\omega'_{y,B}$ at that field. Because the $\omega_\theta$ measurement precision is comparable with the frequency shift $\delta\omega_{y,B}$, the result is consistent with both $\omega_{y,B}$ and $\omega'_{y,B}$.

The small elastic scattering cross section between the two species allows us to rule out collisional hydrodynamics for this observation and instead favor superfluid hydrodynamics as the cause. We interpret the tilt angle modulation as the excitation of a scissors mode of oscillation in the bosonic component driven by interaction with the fermionic component. In trapped atomic systems, the scissors mode is a small amplitude angular oscillation about a principal trap axis, and has previously been utilized to demonstrate and study superfluidity in ultracold atomic gases [41–44]. While the resulting flow is irrotational, the superfluid acquires angular momentum that oscillates at the same frequency as the in-trap angle $\theta_B(t)$ [18].

Our observations imply the existence of a horizontal offset between the two cloud centers which provides a finite impact parameter and therefore nonzero torque during the Yb dipole oscillation [Fig. 3(a)]. In our system, the horizontal cloud offset arises due to a combination of slight angular offsets of both the magnetic field gradient direction and the nearly vertical principal axis of the ODT with respect to the direction of gravity. Since our experimental geometry forces a near degeneracy between the dipole oscillation frequency $\omega_{y,B}$ and that of the scissors mode $\omega_s$, the sinusoidal motion of the Yb center of mass within an offset Li cloud can resonantly drive the scissors mode.

In order to explain the interspecies-interaction-driven scissors mode, we extend the analytical model based on superfluid hydrodynamics developed in Ref. [41] to include the interaction with the fermionic superfluid [18]. The resulting linear-response dynamics for the BEC in-trap tilt angle, $\theta_B$, are identical to those of a sinusoidally driven harmonic oscillator,

$$\frac{d^2\theta_B}{dt^2} = -\omega_s^2\theta_B + g(x_0, y_0)\omega_{x,B}^2 \cos(\omega'_{y,B}t), \qquad (2)$$

where $\omega_s = (\omega_{y,B}^2 + f(x_0)\omega_{x,B}^2)^{1/2}$, $x_0$ is the fixed horizontal cloud displacement, and $y_0$ is the in-trap amplitude of the vertical dipole oscillation. The functions $f$ and $g$ encompass the interspecies interaction effects over the BEC density distribution. Since $|f|$ is at most of order unity [18], $\omega_s \approx \omega_{y,B}$, which clearly reveals the near-resonant nature of the sinusoidal drive.

In this treatment we neglect backaction onto the Li cloud since the Yb angular oscillation frequency is far detuned from the corresponding scissors mode in Li. This implies that the angular momentum imparted to Li from the interaction with Yb is adiabatically transferred to the trap. This effect and the dynamics in Eq. (2) are reproduced in a full numerical simulation of the coupled superfluid dynamics [45].

The observed scissors mode amplitude in Fig. 3 is consistent with a response at the driving frequency $\omega'_{y,B}$, but does not display the linear growth of amplitude in time as one would expect from Eq. (2). We interpret this to be indicative of damping in the scissors mode. Thus, in order to apply our model to the observations, we add a heuristic damping term $-\omega_s\dot{\theta}_B/Q_s$ to the right-hand side of Eq. (2), where $Q_s$ is the quality factor of the scissors mode. We then find that our model reproduces the amplitude observed in Fig. 3(c) for a displacement of roughly twice the Yb Thomas-Fermi radius and $Q_s = 4$ [18]. Furthermore, for this displacement our model predicts the driving force at 720 G to be only 10%–20% larger than that at 780 G, which is consistent with Fig. 3(d).

We have analyzed the consequences of a horizontal offset between the cloud centers for the frequency shift measurements presented in Fig. 2 [18]. On the BEC side of the Feshbach resonance, the mean-field frequency shift is surprisingly robust to horizontal cloud displacement. For the horizontal cloud displacement inferred from the scissors analysis above, the predicted frequency shift becomes 1.5(2)%, which agrees with the value extracted from the measurements in Fig. 2. Our dipole oscillation measurements are therefore consistent with the simultaneous

observation of the driven scissors mode, and with the model discussed above.

In conclusion, we have established a stable two-element Bose-Fermi superfluid system of $^{174}$Yb-$^{6}$Li and studied the frequency shift of dipole oscillations and the excitation of a scissors mode due to interspecies interactions. Extension of these methods can allow investigation of higher order excitations and sound propagation in the dual superfluid [9]. Our experiments also highlight the use of the differences in mass and electronic structure for the selective excitation and controlled spatial overlap of the components, opening new perspectives for investigating the phase diagram of the Bose-Fermi superfluid system [16,46,47].

We thank Martin Zwierlein and Michael McNeil Forbes for useful discussions and critical reading of the manuscript, and the authors of Refs. [31,32] for providing us with their data. This work was supported by NSF Grant No. PHY-1306647, AFOSR Grant No. FA 9550-15-1-0220, and ARO MURI Grant No. W911NF-12-1-0476.

*Note added.*—Recently, we became aware of the realization of a two species mixture of Bose-Fermi superfluids in a $^{41}$K-$^{6}$Li system [48].

[1] I. Bloch, J. Dalibard, and W. Zwerger, Rev. Mod. Phys. **80**, 885 (2008).
[2] M. Anderson, J. R. Ensher, M. R. Matthews, C. E. Wieman, and E. A. Cornell, Science **269**, 198 (1995).
[3] K. B. Davis, M.-O. Mewes, M. R. Andrews, N. J. van Druten, D. S. Durfee, D. M. Kurn, and W. Ketterle, Phys. Rev. Lett. **75**, 3969 (1995).
[4] *The BCS-BEC Crossover and the Unitary Fermi Gas*, Lecture Notes in Physics, edited by W. Zwerger (Springer, Berlin, 2012), Vol. 836.
[5] J. Tuoriniemi, J. Martikainen, E. Pentti, A. Sebedash, S. Boldarev, and G. Pickett, J. Low Temp. Phys. **129**, 531 (2002).
[6] J. Rysti, J. Tuoriniemi, and A. Salmela, Phys. Rev. B **85**, 134529 (2012).
[7] I. Ferrier-Barbut, M. Delehaye, S. Laurent, A. Grier, M. Pierce, B. Rem, F. Chevy, and C. Salomon, Science **345**, 1035 (2014).
[8] A. Andreev and E. Bashkin, Zh. Eksp. Teor. Fiz. **69**, 319 (1975).
[9] G. Volovik, V. Mineev, and I. Khalatnikov, Sov. Phys. JETP **69**, 675 (1975).
[10] T. Ozawa, A. Recati, M. Delehaye, F. Chevy, and S. Stringari, Phys. Rev. A **90**, 043608 (2014).
[11] W. Zheng and H. Zhai, Phys. Rev. Lett. **113**, 265304 (2014).
[12] R. Zhang, W. Zhang, H. Zhai, and P. Zhang, Phys. Rev. A **90**, 063614 (2014).
[13] X. Cui, Phys. Rev. A **90**, 041603(R) (2014).
[14] J. J. Kinnunen and G. M. Bruun, Phys. Rev. A **91**, 041605 (R) (2015).
[15] Y. Castin, I. Ferrier-Barbut, and C. Salomon, C.R. Phys. **16**, 241 (2015).
[16] M. Tylutki, A. Recati, F. Dalfovo, and S. Stringari, New J. Phys. **18**, 053014 (2016).
[17] A. H. Hansen, A. Y. Khramov, W. H. Dowd, A. O. Jamison, B. Plotkin-Swing, R. J. Roy, and S. Gupta, Phys. Rev. A **87**, 013615 (2013).
[18] See Supplemental Material at http://link.aps.org/supplemental/10.1103/PhysRevLett.118.055301 for an expanded discussion on the two-species superfluid mixture preparation and characterization, the derivation of the driven-scissors model and associated discussion of the role of angular momentum, and the calculation of the effect of horizontal cloud displacement on the bosonic dipole frequency shift, which includes Refs. [19–27].
[19] A. T. Grier, I. Ferrier-Barbut, B. S. Rem, M. Delehaye, L. Khaykovich, F. Chevy, and C. Salomon, Phys. Rev. A **87**, 063411 (2013).
[20] A. Burchianti, G. Valtolina, J. A. Seman, E. Pace, M. De Pas, M. Inguscio, M. Zaccanti, and G. Roati, Phys. Rev. A **90**, 043408 (2014).
[21] F. Sievers, N. Kretzschmar, D. R. Fernandes, D. Suchet, M. Rabinovic, S. Wu, C. V. Parker, L. Khaykovich, C. Salomon, and F. Chevy, Phys. Rev. A **91**, 023426 (2015).
[22] A. Y. Khramov, A. H. Hansen, A. O. Jamison, W. H. Dowd, and S. Gupta, Phys. Rev. A **86**, 032705 (2012).
[23] F. Dalfovo, S. Giorgini, L. P. Pitaevskii, and S. Stringari, Rev. Mod. Phys. **71**, 463 (1999).
[24] M. Ku, Ph.D. thesis, Massachusetts Institute of Technology, 2015.
[25] M. Edwards, C. W. Clark, P. Pedri, L. Pitaevskii, and S. Stringari, Phys. Rev. Lett. **88**, 070405 (2002).
[26] M. Modugno, G. Modugno, G. Roati, C. Fort, and M. Inguscio, Phys. Rev. A **67**, 023608 (2003).
[27] O. Marago, G. Hechenblaikner, E. Hodby, S. Hopkins, and C. Foot, J. Phys. Condens. Matter **14**, 343 (2002).
[28] R. Roy, A. Green, R. Bowler, and S. Gupta, Phys. Rev. A **93**, 043403 (2016).
[29] C.-L. Hung, X. Zhang, N. Gemelke, and C. Chin, Phys. Rev. A **78**, 011604(R) (2008).
[30] N. Navon, S. Nascimbène, F. Chevy, and C. Salomon, Science **328**, 729 (2010).
[31] M. J. H. Ku, A. T. Sommer, L. W. Cheuk, and M. Zwierlein, Science **335**, 563 (2012).
[32] R. Haussmann and W. Zwerger, Phys. Rev. A **78**, 063602 (2008).
[33] D. S. Petrov, C. Salomon, and G. V. Shlyapnikov, Phys. Rev. Lett. **93**, 090404 (2004).
[34] L. D. Carr, G. V. Shlyapnikov, and Y. Castin, Phys. Rev. Lett. **92**, 150404 (2004).
[35] G. Zürn, T. Lompe, A. N. Wenz, S. Jochim, P. S. Julienne, and J. M. Hutson, Phys. Rev. Lett. **110**, 135301 (2013).
[36] We perform a separate measurement of the stability of the dual superfluid at 780 G in the dipole oscillation trap conditions and confirm that the data in Fig. 2 is well within a single $1/e$ decay time.
[37] M. Delehaye, S. Laurent, I. Ferrier-Barbut, S. Jin, F. Chevy, and C. Salomon, Phys. Rev. Lett. **115**, 265303 (2015).
[38] V. V. Ivanov, A. Khramov, A. H. Hansen, W. H. Dowd, F. Münchow, A. O. Jamison, and S. Gupta, Phys. Rev. Lett. **106**, 153201 (2011).

[39] H. Hara, Y. Takasu, Y. Yamaoka, J. M. Doyle, and Y. Takahashi, Phys. Rev. Lett. **106**, 205304 (2011).

[40] For the magnitude of $a_{BF}$, we use a weighted mean of the values reported in Refs. [38,39].

[41] D. Guery-Odelin and S. Stringari, Phys. Rev. Lett. **83**, 4452 (1999).

[42] O. M. Marago, S. A. Hopkins, J. Arlt, E. Hodby, G. Hechenblaikner, and C. J. Foot, Phys. Rev. Lett. **84**, 2056 (2000).

[43] G. Modugno, M. Modugno, F. Riboli, G. Roati, and M. Inguscio, Phys. Rev. Lett. **89**, 190404 (2002).

[44] M. J. Wright, S. Riedl, A. Altmeyer, C. Kohstall, E. R. Sanchez Guajardo, J. H. Denschlag, and R. Grimm, Phys. Rev. Lett. **99**, 150403 (2007).

[45] Work in collaboration with the theory group of Michael McNeil Forbes (to be published).

[46] A. B. Kuklov and B. V. Svistunov, Phys. Rev. Lett. **90**, 100401 (2003).

[47] B. Ramachandhran, S. G. Bhongale, and H. Pu, Phys. Rev. A **83**, 033607 (2011).

[48] X. C. Yao, H. Z. Chen, Y. P. Wu, X. P. Liu, X. Q. Wang, X. Jiang, Y. Deng, Y. A. Chen, and J. W. Pan, Phys. Rev. Lett. **117**, 145301 (2016).